Applied Surface Science 670 (2024) 160719

Contents lists available at ScienceDirect

Applied Surface Science

journal homepage: www.elsevier.com/locate/apsusc

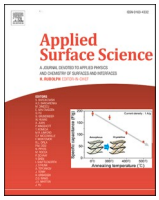

Full Length Article

Physico-chemical characterization of polyimide passivation layers for high power electronics applications

Valentina Spampinato [a,*], Alessandro Auditore [a], Nunzio Tuccitto [a], Roberta Vitale [b], Gabriele Bellocchi [b], Francesco Galliano [b], Simone Rascunà [b], Giuseppe Arena [b], Antonino Licciardello [a]

[a] Department of Chemical Sciences, University of Catania and Center for Colloid and Surface Science (CSGI), Viale A. Doria 6, 95125 Catania, Italy
[b] STMicroelectronics, Stradale Primosole 50, I-95121 Catania, Italy

ARTICLE INFO

Keywords:
Time-of-flight secondary ion mass spectrometry
Argon cluster depth profile
Polyimide
Passivation layer
Power electronics
Silicon carbide

ABSTRACT

Silicon carbide (SiC) is a wide bandgap semiconductor suitable for high-voltage, high-power and high-temperature applications. However, the production of advanced SiC power devices still remains limited due to some shortcomings of the dielectric properties of the passivation layer. Thanks to their high operating temperature and dielectric strength, spin coated polyimide (PI) layers are considered ideal candidates for SiC devices passivation and insulation. In this view, a robust methodology for the physico-chemical characterization of such PI layers is required. Thanks to the use of time of flight-secondary ion mass spectrometry (ToF-SIMS), a SIMS-based surface-sensitive technique that provides specific identification of molecules, it was possible to distinguish different types of PIs employed in commercial SiC devices and postulate their molecular structure. This was obtained after careful selection of the analytical conditions used for the characterization of the specimens.

The results attained in this study open the way for further improvements in one of the most key issues in the development of higher SiC power devices.

1. Introduction

Silicon carbide (SiC) stands out as a promising wide bandgap semiconductor, well-suited for demanding applications characterized by high voltage, power, and temperature requirements [1,2]. However, the full potential of advanced SiC power devices has been hindered by limitations in the dielectric properties of the passivation layer [3].

With the aim of ensuring the reliability of the power device, electrical insulation is essential.

The passivation layer used must have specific characteristics to sustain the performance of the device for the entire planned life cycle: excellent dielectric properties, stability at operating temperature, and the ability to protect the device from the external environment. Moreover, these devices are tested under stress conditions and the passivation layer response to the stress not only depends on the thermo-mechanical properties, but also on the interaction at the interface between the molding compound and the organic material. Therefore, a deep knowledge of the passivation layers' properties and interaction with the interfaces is crucial to design robust SiC power devices.

Organic dielectrics are considered to be low-cost and with good processing characteristics. Among organic dielectric materials, polyimides (PIs) are a well-known class of insulator polymers employed as passivation layer [4]. The possibility to introduce lateral groups and functional moieties in their chemical structure allows for the tuning of their properties on demand, such as mechanical properties like tensile strength, thermal properties like coefficient of thermal expansion, and adhesive properties. All these are crucial properties in the design of an efficient SiC power device. For instance, PIs bearing in their chemical structure heterocyclic imide rings have shown outstanding thermal and electrical properties even at high temperatures [5]. It is therefore clear that, in order to gather information on the properties and the interactions of the PI employed in the device, knowledge of its molecular structure is paramount.

This study is driven by the objective of identifying the most

Abbreviations: SiC, silicon carbide; PI, polyimide; ToF-SIMS, time-of-flight secondary ion mass spectrometry; GCIB, gas cluster ion beam; PCA, principal component analysis; SR, sputter rate; SY, sputter yield; PBO, polybenzoxazole; PAI, polyamideimide; PEI, polyetherimide.

* Corresponding author.
E-mail address: valentina.spampinato@unict.it (V. Spampinato).

https://doi.org/10.1016/j.apsusc.2024.160719
Received 10 May 2024; Received in revised form 4 July 2024; Accepted 9 July 2024
Available online 11 July 2024

appropriate analytical conditions to facilitate a comparative analysis of various PI layers already integrated into commercial SiC devices. Employing time-of-flight secondary ion mass spectrometry (ToF-SIMS), a robust and surface-sensitive technique, the research seeks to discriminate among layers composed by different PIs and postulate their molecular structure.

ToF-SIMS is one of the most suitable characterization techniques to study the surface composition of a large variety of materials. This is thanks to its surface sensitivity, high mass and lateral resolution, and the possibility to collect both elemental and molecular information. When used in static mode (typical limit fluence $< 10^{12}$ ion/cm^2) [6] the technique is able to sample the outermost layer (i.e. < 2–3 nm). This, in most cases, is a great advantage of the technique. However, in other cases, it could be a drawback. In fact, if the samples are not freshly prepared or some of the processes lead to some kind of contamination, the high surface sensitivity will allow the detection only of the contaminants, burying the information on the layer of interest.

In the case of high surface contamination, different approaches should be preferred in order to obtain a clear understanding of the studied samples. One approach would involve the analysis of the samples in depth, by alternating a sputter cycle to an analysis cycle so that the first would remove one layer at a time allowing the analysis beam to characterize a "fresh" surface at each cycle. One of the most traditional sputter sources in the analysis of materials with application in microelectronics, as in this case, is the Cs^+ beam. Although Cs^+ has been proven to be an interesting sputter beam for hybrid materials [7], it is still not entirely performant if one wants to retain the molecular information. In fact, besides C and small C-based fragments, unless very low energy (~200 eV) is used [8], usually Cs^+ sputtering does not allow to follow molecular or quasi-molecular fragments due to damage accumulation during depth profiling [9]. This is, surely, one significant drawback of this kind of sputter beam and many efforts have been spent in the last years to overcome it. Among different attempts to circumvent the molecular information loss during sputtering of organic, C_{60}^+ played a valuable role [10]. However, this approach was demonstrated to be successful mostly for polymers mainly characterized by an ion beam-induced chain-scission degradation process, such as polymethylmethacrylate [11]. Indeed, polymers which have the tendency to crosslink, such as polystyrene, could not maintain their molecular structure under bombardment, leading to the emission of small carbon-based fragments only. A way to assist the sputtering via C_{60}^+ and aid the molecular information is the use of a radical scavenger during the sputtering, such as NO dosing [12,13], but also in this case the success of the approach strictly depends on the nature of the investigated material.

The most successful attempt to overcome the high fragmentation damage induced by SIMS on organic species is without doubt the introduction of the large Ar gas cluster ion beam (Ar GCIB) [14–16]. Thanks to its cluster nature, with clusters typically between 500 and 5000 atoms, the impact on the surface of a cluster formed by n Ar atoms can be regarded, as a first approximation and neglecting nonlinear effects that are in fact present, as the impact of individual atoms each of them carrying 1/n of the energy of the whole cluster. This allows a much gentler interaction between the beam and the material, granting the possibility to extract entire molecules and large fragments. This is of course of utmost importance when one needs to discriminate among different organic materials with very similar chemical structure.

Another approach, which still benefits of the advent of large gas cluster ion beams, would involve a gentle cleaning process via Ar cluster in order to remove the contamination layer. Of course, should the contaminants be mainly related to inorganics, this approach would be less effective, since Ar cluster beams are usually not efficient for the sputtering of inorganic materials.

It should be mentioned that the ToF-SIMS technique generates complex, high-dimensional data sets with spectra containing thousands of mass-to-charge ratio peaks. Yet it is within this complexity that interesting and complete information about the analyzed sample is contained. In order to extract clear and useful information from these complex data sets, the application of multivariate analysis (MVA) techniques can be crucial. Among those, Principal Component Analysis (PCA) aims at simplifying complex data sets by reducing their dimensionality while preserving most of the variance [17] and it has been successfully applied in several studies involving ToF-SIMS analysis [18–20].

Indeed, PCA identifies patterns within the spectra generated during a ToF-SIMS experiment by transforming the original correlated variables (mass peaks) into a new set of uncorrelated variables called "principal components". These components are linear combinations of the original variables and are ordered such that the first few retain most of the variation present in the original data set. This reduction in dimensionality facilitates the interpretation and visualization of the ToF-SIMS data, helping to identify underlying trends, differentiate between sample types, and highlight significant features that may correspond to specific chemical compounds or surface properties.

In this work, a robust approach to characterize thick polymeric-based passivating layers with applications in microelectronics that combines dual beam SIMS investigation with PCA multivariate analysis is presented. The proposed approach allowed to identify polyimides with unknown structures and find similarities and differences among the studied layers. This research marks a significant stride forward, addressing a key obstacle in SiC power device evolution. The insights gained not only contribute to a deeper understanding of polyimide functionalities in SiC applications but also offer a foundation for future enhancements, fostering the continuous progress of SiC technology.

2. Materials and methods

Commercial devices were used as source samples for the polyimide-based passivation layers; the reference PI, a fluorinated polybenzoxazole, was deposited by spin coating on a blanket silicon wafer and cured in a nitrogen atmosphere.

The SIMS experiments were carried out using a time-of-flight SIMS (ToF-SIMS) instrument (ToF-SIMS IV, ION-TOF GmbH, Münster, Germany). As analysis beam, 25 keV bismuth primary ions produced by a liquid metal ion gun was used. The surface spectra were acquired in positive polarity mode using Bi_3^+ primary ions from square areas of 200 × 200 μm^2 in high current bunched mode (resolution M/ΔM ~ 8000 at *m/z* 29), with a beam spot size of ~ 2.5 μm. During the dual beam depth profile experiments, two different sputter beams were used: (i) a Cs^+ at either 3 keV or 1 keV, rastered over 100 × 100 μm^2 and (ii) a Ar_{4000}^+ GCIB at 20 keV, rastered over 400 × 400 μm^2. The analysis beam for the dual beam depth profiles was the same as for the surface spectra, with the rastered areas adjusted at 50 × 50 μm^2 for the Cs^+ experiments, and 200 × 200 μm^2 for the GCIB experiment. During the analysis, a low-energy (~20 eV) electron flood gun was used to prevent charging of the surface. Spectral interpretation was carried out using SurfaceLab software v7.2 (ION-TOF GmbH, Münster, Germany).

PCA was performed on the collected datasets using the NESAC/BIO MVA Toolbox (Spectragui v2.7 standalone, https://www.nb.engr.washington.edu/mvsa/nbtoolbox). Prior to PCA analysis, a data preprocessing step was applied to the dataset to remove variance that is not due to chemical differences between the samples. Specifically, the mass spectra were first normalized to the sum of selected peaks, to account for fluctuations in secondary ion yield between different spectra and then SQRT-mean-centered.

3. Results and discussion

3.1. Finding the ideal conditions to maximize molecular information

The PI layers were characterized via ToF-SIMS in static mode, in order to study the surface composition. As already mentioned, this approach allows to detect elements and components only from the

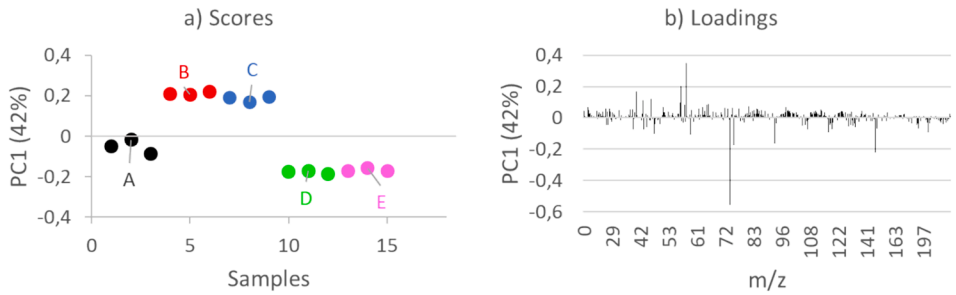

Fig. 1. PCA scores (a) and loadings (b) plots related to the surface spectra obtained from the five studied PI layers (A, B, C, D and E).

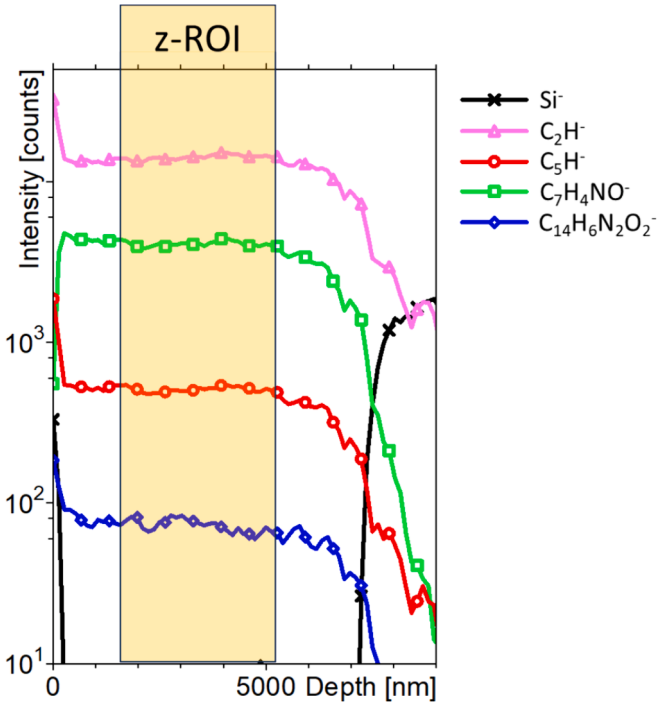

Fig. 2. Representative dual beam depth profile of the reference PI. The yellow region indicates a representative z-ROI from which mass spectra are reconstructed.

outermost layer (i.e. < 2–3 nm), thanks to the high surface sensitivity of the technique. Unfortunately, with this approach, only surface contaminants were detected, probably due to strong contamination at the top surface introduced during the device fabrication. Indeed, unsupervised multivariate analysis, namely PCA, was carried out on those spectra recorded on the outermost layer of the samples and the largest variance was observed for polysiloxane fragments [21] such as $SiC_2H_7^+$ (*m/z* 59), $SiC_3H_9^+$ (*m/z* 73), $Si_2C_5H_{15}O_3^+$ (*m/z* 147) and $Si_3C_5H_{15}O_3^+$ (*m/z* 207), typically related to surface contamination and inorganic contaminants (see Fig. 1).

Given the high surface contamination, a different approach had to be used in order to obtain a clear view on the different PI samples: dual beam depth profile analysis. This approach, as previously outlined, entails the sequential utilization of two beams: the first, a sputter beam, erodes the sample, and the second, an analysis beam, provides the spectrum of the surface of the crater produced by the sputter beam.

A typical dual beam depth profile (obtained with GCIB sputter beam) of a reference PI with a fluorinated benzoxazole structure is shown in Fig. 2. Some ionic fragments related to the organic layer with general chemical formula $C_xH_y^-$ and $C_xH_yN_zO_w^-$ are displayed, together with Si^- from the substrate. From such a profile one can reconstruct the secondary ion mass spectrum from a chosen depth window ("z-ROI", as indicated in the depth profile depicted in Fig. 2), for instance in order to exclude the outer layers that are affected by contamination. This methodology was indeed employed to extrapolate the mass spectra discussed in this section.

Initially, a Cs^+ sputter beam was used to analyze a PI layer used as reference, since, traditionally, Cs^+ is one of the most commonly used beams for the study of systems related to microelectronics. Two different energies were explored in order to evaluate the difference between a more (3 keV) and a less (1 keV) energetic beam but, unfortunately, in both cases, it was not possible to maintain significant molecular information as – mainly – C and small C-based fragments were detected, as shown in the reconstructed spectra of Fig. 3a, b where the most populated portion is the low mass one.

The failure of the previously described approach suggests severe damage due to the interaction with the Cs^+ ion beam. For this reason, a different sputter beam that has been demonstrated to be efficient in the sputtering of organic materials and polymers was selected: a large Ar gas cluster ion beam (Ar GCIB). As previously mentioned, with a GCIB the total energy of the cluster is divided among the cluster's components, hence generating a much gentler interaction between the ion beam and the material.

The use of the GCIB allowed to gather information about larger C-based mass peaks. In fact, some PI characteristic fragments were detected with much higher intensity than in depth profiling experiments where the Cs^+ sputter beam was used. As shown in Fig. 3c, moving from Cs^+ 3 keV to 1 keV and then to GCIB, the high mass region of the spectrum becomes increasingly more populated. A list of nominal masses of some of the most relevant fragments is reported in Table 1 together with a possible assignment.

As shown in Fig. 3, when comparing the mass spectra integrated over the depth profile obtained with Cs^+ (3 and 1 keV) and Ar GCIB, the ratio between high masses and low masses peaks goes in favor of the high masses in the latter. This is already a clear indication of a much gentler interaction between the GCIB and the sample.

In order to compare the level of chemical information obtained with the two different sputter beams, Fig. 4 displays the intensity ratio of some large fragments of interest, which carry high chemical information content, over that of some smaller (non-specific) fragments obtained from the depth profile measurements of the PI reference, mainly containing C and H. Specifically, as large fragments, the ones at *m/z* 118, *m/z* 234 and *m/z* 580 were considered. They were then normalized to the sum of the intensity of ions with general chemical formula $[C_{n+1}H]^-$ (with $0 \leq n \leq 4$), coming from the PI's backbone fragmentation, and CN^-, characteristic of the imide functional group. The obtained ratio was normalized to the corresponding one obtained with the GCIB. As shown in Fig. 3, the intensity ratio obtained with Cs^+ 3 keV is below 2 % of the one obtained using the cluster beam. The situation does improve when decreasing the energy from 3 keV to 1 keV, however, in this case, the intensity ratio is still low compared to the GCIB one: only 10 %, in the best case. Therefore, the data displayed both in Fig. 3 and Fig. 4 clearly indicate that the highest amount of information is obtained in the GCIB experiment.

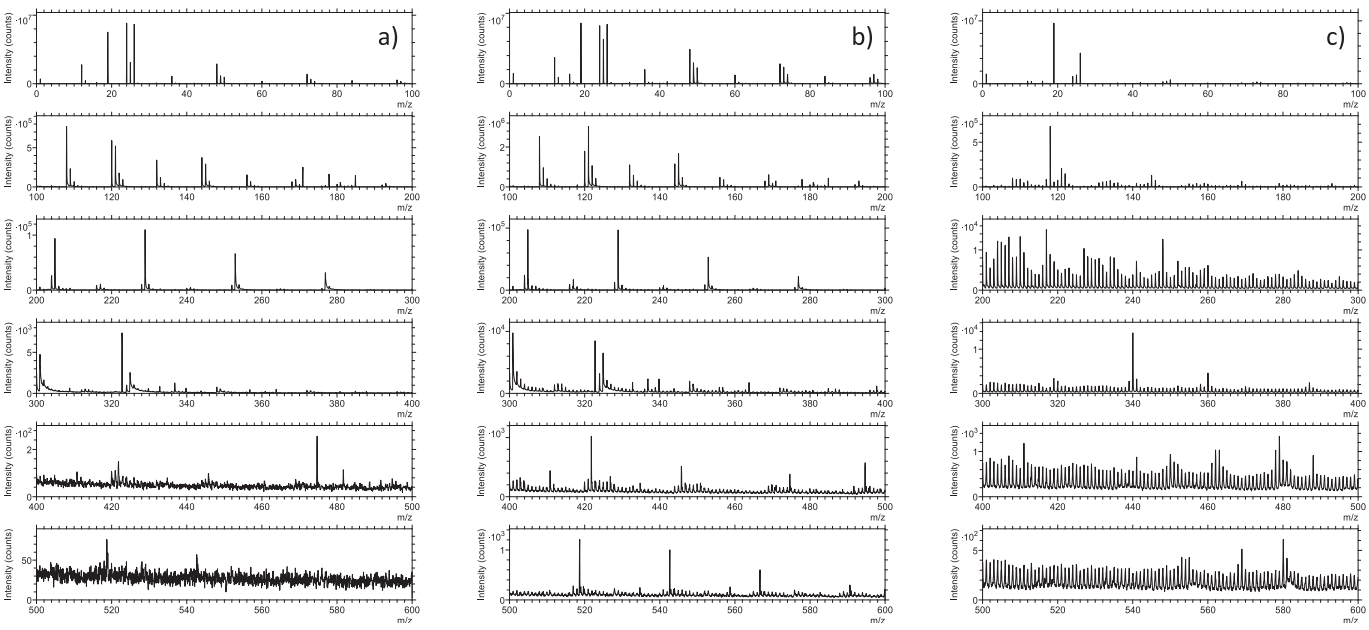

Fig. 3. ToF-SIMS mass spectra of the reference PI integrated over the depth profiles collected with Cs^+ 3 keV (a), Cs^+ 1 keV (b) and Ar GCIB (c).

Table 1
Mass (*m/z*) and possible assignment of some fragments of interest identified for the reference PI.

m/z	Possible assignment	*m/z*	Possible assignment
1	H^-	96	$C_4H_2O_2N^-$
12	C^-	118	$C_7H_4NO^-$
13	CH^-	120	$C_7H_6NO^-$
16	O^-	121	$C_7H_7NO^-$
17	OH^-	144	$C_8H_2O_2N^-$
19	F^-	145	$C_8H_3O_2N^-$
24	C_2^-	146	$C_8H_4O_2N^-$
25	C_2H^-	150	$C_3F_6^-$
26	CN^-	161	$C_8H_3NO_3^-$
28	Si^-	162	$C_8H_4NO_3^-$
31	CF^-	234	$C_{14}H_6N_2O_2^-$
36	C_3^-	235	$C_{14}H_5NO_3^-$
37	C_3H^-	236	$C_{14}H_6NO_3^-$
41	C_2HO^-	237	$C_{14}H_7NO_3^-$
42	CNO^-	309	$C_{20}H_9N_2O_2^-$
48	C_4^-	340	$C_{21}H_9N_2O_2F^-$
49	C_4H^-	360	$C_{21}H_{10}N_2O_2F_2$
60	C_5^-	384	$C_{17}H_6N_2O_2F_6^-$
61	C_5H^-	387	$C_{17}H_9N_2O_2F_6^-$
69	CF_3^-	411	$C_{22}H_{11}N_2O_2F_4^-$
72	C_6^-	441	$C_{23}H_{10}N_2O_2F_5^-$
73	C_6H^-	462	$C_{23}H_{12}N_2O_2F_6^-$
75	$C_6H_3^-$	479	$C_{23}H_{10}N_2O_2F_7^-$
78	$C_6H_6^-$	569	$C_{29}H_{17}N_3O_3F_6^-$
91	$C_6H_3O^-$	580	$C_{30}H_{16}N_3O_3F_6^-$

Moreover, in the choice of the best experimental conditions, one should also take into account the time needed for the measurements, considering that the typical thickness of the PI films under study is rather large, of the order of 5–10 μm. The sputter rate (SR), and the related sputter yield (SY) for the three approaches was experimentally obtained by measuring the crater depth after a certain sputter time and is reported in Table 2. Comparing the data displayed in the table, it becomes clear that, even in terms of measuring time, the GCIB approach results as a preferable choice. Indeed, the large difference between Cs^+ and GCIB might suggest, besides the sputter beam induced damage already mentioned, the tendency of the studied layer to crosslink under the Cs^+ beam, therefore creating an amorphous or carbonized layer which becomes harder to remove during sputtering. Therefore, it was concluded

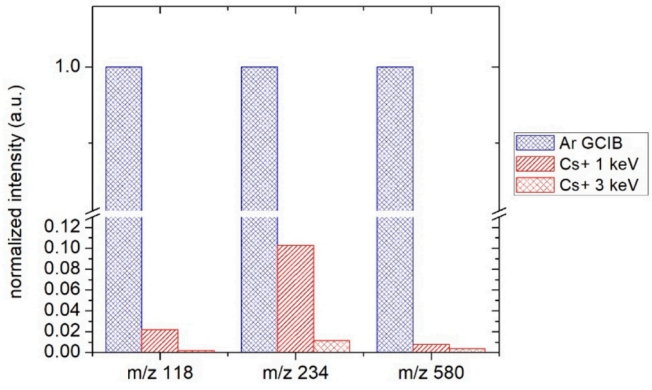

Fig. 4. Intensity ratios of mass peaks of interest for Cs^+ 1 keV and 3 keV normalized to the GCIB ratios. The normalization applied is explained in detail in the text.

Table 2
Sputter rates (SR) and sputter yields (SY) calculated on the PI reference for different sputter beams.

	Energy (keV)	Raster size (μm)	Current (nA)	SR (nm/s)	SY (nm^3/ions)
Cs^+	1	100 × 100	~18	~0.08	~0.007
Cs^+	3	100 × 100	~32	~0.82	~0.041
Ar^+_{4000}	20	200 × 200	~2.6	~10.5	~25.95

that the best methodology to study this kind of film was the GCIB depth profile approach.

3.2. Physico-chemical characterization of different PI layers

Having identified suitable conditions to characterize the PI reference layer, the study could focus on the analysis of different kinds of PI with unknown chemical structure. In this case, the aim of the study was to find chemical differences among five different PIs used in the microelectronic industry. In fact, the choice of a particular PI-based passivation layer is driven by several factors such as the resilience to thermal,

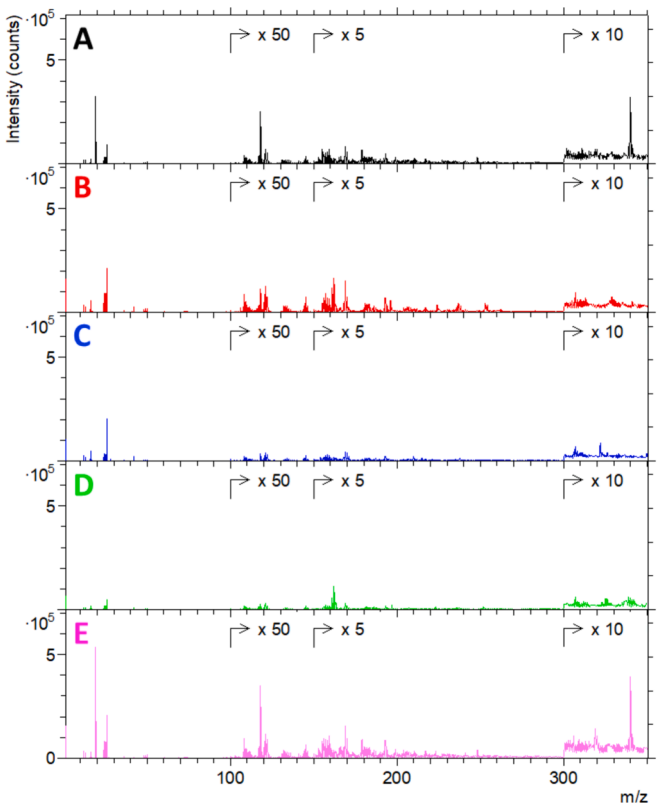

Fig. 5. Overlay of the ToF-SIMS mass spectra integrated over the depth profiles of the five studied PI layers.

electrical and mechanical stresses as well as process compatibility issues. Both the choice of the PI passivation layer and the understanding of potential failure mechanisms require a thorough knowledge of the chemical nature of these layers.

Depth profiles for each of the five PI layers, namely A, B, C, D, E, were acquired ensuring that for all the samples high-masses fragments were detected with reasonable intensity. Then, the first datapoints in the depth profiles, which are affected by surface contamination (as proved in Section 3.1), were excluded and, for each sample, a mass spectrum was reconstructed from the same depth range of the film, i.e. similar z-ROI, as described in Section 3.1. In Fig. 5, the overlay of the mass spectra integrated over the same z-ROI is reported, showing some differences in the fragmentation pattern of the five compared samples. For example, the peak at *m/z* 118 and the one at *m/z* 340 appear to be more intense for samples A and E, while the peak at *m/z* 162 shows a higher intensity in samples B and D.

Due to the large amount of data generated by a ToF-SIMS analysis, it was decided to carry out PCA on the collected datasets. To do so, a peak list containing almost 80 % of the mass peaks composing the depth profiles was generated and applied to the five studied samples. The results, depicted as score plots and loadings, are reported in Fig. 6. The first principal component (PC1) is able to explain almost 94 % of the variance in the dataset and it clearly discriminates samples A and E from samples B, C and D. From the loadings, it is noted that fluorine is the main variable that characterizes samples A and E, together with CF_3^- (*m/z* 69) and $C_7H_4NO^-$ (*m/z* 118), while carbon-, oxygen- and nitrogen-based fragments are more relevant for the other samples. Specifically, C_2HO^- (*m/z* 41), CNO^- (*m/z* 42), $C_6H_3O^-$ (*m/z* 91) and $C_8H_4NO_3^-$ (*m/z* 162) seem to be more distinctive for sample B and D. Sample C is mainly characterized by C^-, O^- and CN^-.

Focusing the attention on the high-mass peaks identified by the PCA, it was possible to recognize some monomers or large fragments related to possible PI structures used in microelectronics [22–25]. Particular attention was paid to two fragments, one at *m/z* 118 and the other one at *m/z* 162. From a thorough study of all the possible PI structures that could lead to those two fragments, it was found that polybenzoxazole (PBO) contains the oxazole moiety whose chemical formula is C_7H_4NO (*m/z* 118), while polyimide (Upilex), polyamideimide (PAI) and polyetherimide (PEI) contain the imide moiety with chemical formula $C_8H_4O_2N$ (*m/z* 146), as shown in Fig. 7.

As displayed in Fig. 8, the fragment related to the oxazole moiety

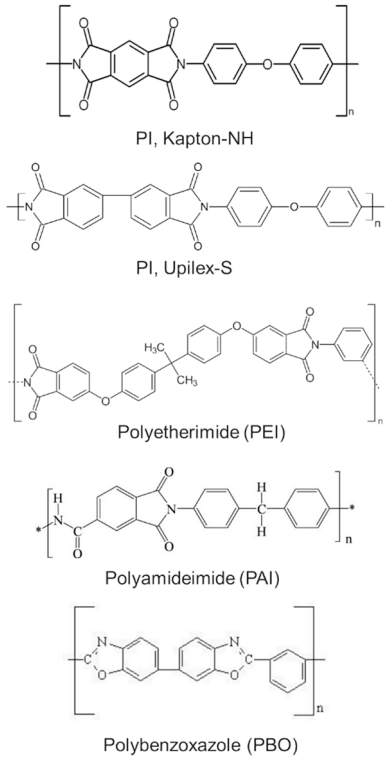

Fig. 7. Chemical structures of some polyimide-based polymers used in microelectronics.

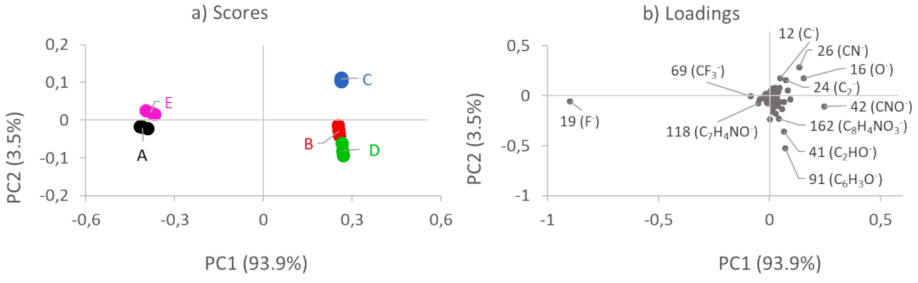

Fig. 6. PCA scores (a) and loadings (b) plots related to the mass spectra integrated over the z-ROIs in the depth profiles of the five studied PI layers (A, B, C, D and E).

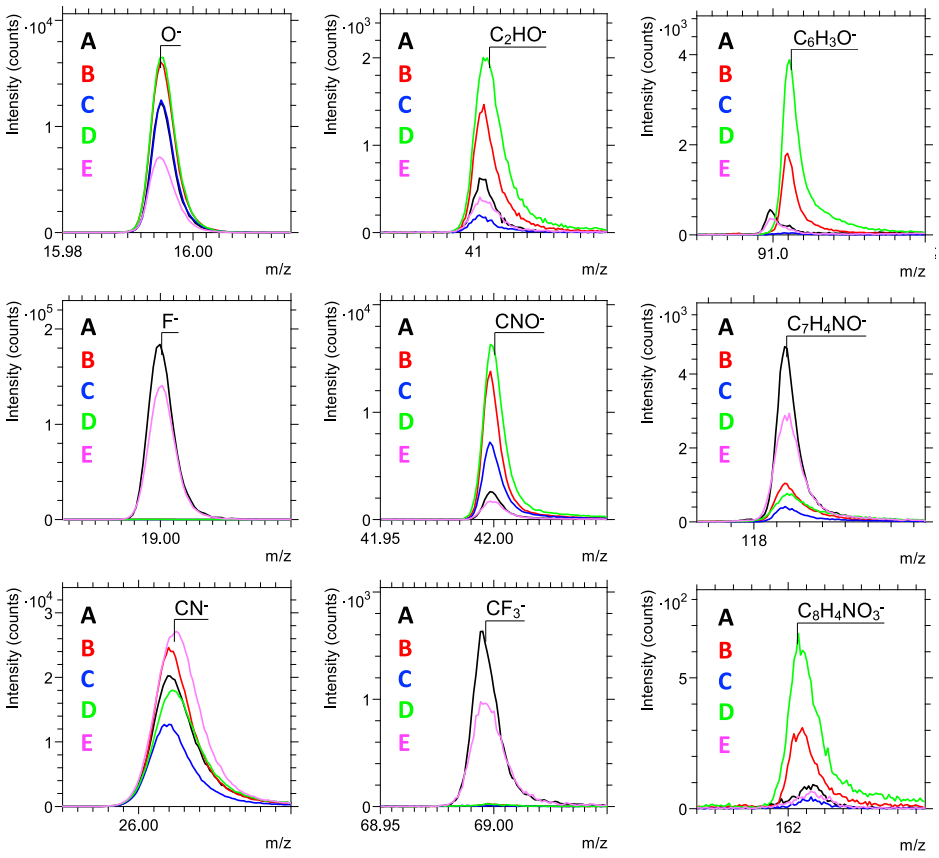

Fig. 8. ToF-SIMS mass spectra overlay of specific mass ranges related to some negative ions of interest.

($C_7H_4NO^-$) was detected in negative polarity mode with higher intensity in samples A and E, together with smaller fragments such as CF^- and CF_3^-. Therefore, a structure of the layer such as a PBO backbone with a C $(CF_3)_2$ group positioned between the two oxazole groups was postulated. Indeed, large fragments, such as $C_{17}H_9N_2O_2F_6^-$ at *m/z* 387, $C_{23}H_{12}N_2O_2F_6^-$ at *m/z* 462 and $C_{30}H_{16}N_3O_3F_6^-$ at *m/z* 580, compatible with the fragmentation of the proposed structure were detected in the mass spectra of the two samples, A and E. These fragments can match a chemical structure with two or three oxazole moieties connected by a C $(CF_3)_3$ and a benzene ring.

As reported in Fig. 8, samples B and D, shown higher intensities for fragments such as $C_6H_3O^-$ (*m/z* 91) and $C_8H_4O_3N^-$ (*m/z* 162), which strongly support a chemical structure similar to the PEI one, where the imide moiety is bound to the benzene ring via an oxygen atom. This would exclude a layer composition related to Upilex or PAI structures.

These findings confirm what was observed in the PCA, leading to the conclusion that a similar PI formulation was used for samples A and E, on one hand (i.e. a CF_3 modified PBO), and sample B and D, on the other hand (i.e. a PEI). The formulation of sample C is less clear, and it might be related to a passivation layer with a molecular structure in between the two postulated for the other samples.

4. Conclusions

In this study, a ToF-SIMS approach for the characterization of thick polymeric layers with interest in the microelectronic field is presented. The study demonstrated that even though static spectra, in principle, would be sufficient to provide information on the nature of the passivation layers, the surface contamination deriving from diverse processes needed in the fabrication of the microelectronics device may hide such information. On the other hand, traditional approaches involving sputter profiling of such layers by means of ion beams, such as Cs^+, did not allow the retention of the molecular information during the analysis. Thanks to the application of large gas cluster sources, in this case Ar^+_{4000}, it was possible to detect large fragments, attributable to specific polymeric structures, along the sample depth. This allowed to discriminate different unknown polyimide-based passivation layers, identify differences and similarities among them and hypothesize their chemical structures, also with the help of multivariate analysis.

This approach can be regarded as a robust methodology for the chemical characterization of different polymeric layers of relevance in technological applications, such as passivation layers, especially in those cases where the molecular structure is not known and must be determined.

CRediT authorship contribution statement

Valentina Spampinato: Writing – review & editing, Writing – original draft, Validation, Supervision, Project administration, Methodology, Investigation, Funding acquisition, Formal analysis, Data curation, Conceptualization. **Alessandro Auditore:** Writing – review & editing, Validation, Investigation, Conceptualization. **Nunzio Tuccitto:** Writing – review & editing, Conceptualization. **Roberta Vitale:** Writing – review & editing. **Gabriele Bellocchi:** Writing – review & editing, Resources. **Francesco Galliano:** Resources. **Simone Rascunà:** Resources. **Giuseppe Arena:** Supervision, Resources. **Antonino Licciardello:** Writing – review & editing, Supervision, Resources, Conceptualization.

Declaration of competing interest

The authors declare that they have no known competing financial interests or personal relationships that could have appeared to influence the work reported in this paper.

Data availability

Data will be made available on request.

Acknowledgements

This work was supported by the project MetTriPI (Metodologie avanzate per la caratterizzazione chimico fisica Tridimensionale di sistemi Polimerici ed Ibridi), founded by PIano di inCEntivi per la RIcerca (PIACERI) 2020/2022, Linea di Intervento 3 “Starting Grant”, Università degli Studi di Catania. The authors would like to acknowledge Dr. D. Graham (NESLAB, University of Washington, USA) for providing the MVA toolbox used for the PCA data analysis.

References

[1] A. Elasser, T.P. Chow, Silicon carbide benefits and advantages for power electronics circuits and systems, Proceedings of the IEEE 90 (2002) 969–986, https://doi.org/10.1109/JPROC.2002.1021562.
[2] T. Kimoto, Material science and device physics in SiC technology for high-voltage power devices, Jpn. J. Appl. Phys. 54 (2015) 040103, https://doi.org/10.7567/JJAP.54.040103.
[3] S. Zelmat, M.-L. Locatelli, T. Lebey, S. Diaham, Investigations on high temperature polyimide potentialities for silicon carbide power device passivation, Microelectron. Eng. 83 (2006) 51–54, https://doi.org/10.1016/j.mee.2005.10.050.
[4] C.P. Wong (Ed.), Polymers for Electronic and Photonic Applications, Academic Press Inc., London, 1993.
[5] Q.-H. Lu, F. Zheng, Chapter 5 - Polyimides for Electronic Applications in: Shi-Yong Yang (Ed.), Advanced Polyimide Materials, Elsevier, 2018, 195-255. https://doi.org/10.1016/B978-0-12-812640-0.00005-6.
[6] A. Benninghoven, Chemical analysis of inorganic and organic surfaces and thin films by static time-of-flight secondary ion mass spectrometry (TOF-SIMS), Angew. Chem. Int. Ed. Engl. 33 (1994) 1023-1043. https://doi.org/10.1002/anie.199410231.
[7] C. Noël, L. Houssiau, Hybrid organic/Inorganic materials depth profiling using low energy cesium ions, J. Am. Soc. Mass. Spectrom. 27 (2016) 908–916. https://doi.org/10.1007/s13361-016-1353-9.
[8] L. Houssiau, B. Douhard, N. Mine, Molecular depth profiling of polymers with very low energy ions, Appl. Surf. Sci. 255 (2008) 970–972, https://doi.org/10.1016/j.apsusc.2008.05.027.
[9] T. Terlier, G. Zappalà, C. Marie, D. Leonard, J.-P. Barnes, A. Licciardello, ToF-SIMS depth profiling of PS-b-PMMA block copolymers using Ar_n^+, C_{60}^{++}, and Cs^+ sputtering Ions, Anal. Chem. 89 (2017) 6984–6991, https://doi.org/10.1021/acs.analchem.7b00279.
[10] A. Wucher, J. Cheng, N. Winograd, Molecular depth profiling using a C(60) cluster beam: the role of impact energy, J. Phys. Chem. C: Nanomaterials and Interfaces 112 (2008) 16550–16555, https://doi.org/10.1021/jp8049763.
[11] R. Möllers, N. Tuccitto, A. Torrisi, E. Niehuis, A. Licciardello, Chemical effects in C_{60} irradiation of polymers, Appl. Surf. Sci. 252 (2006) 6509–6512, https://doi.org/10.1016/j.apsusc.2006.02.083.
[12] G. Zappalà, V. Motta, N. Tuccitto, S. Vitale, A. Torrisi, A. Licciardello, Nitric oxide assisted C_{60} secondary ion mass spectrometry for molecular depth profiling of polyelectrolyte multilayers, Rapid Commun. Mass Spectrom. 29 (2015) 2204–2210, https://doi.org/10.1002/rcm.7383.
[13] R. Havelund, A. Licciardello, J. Bailey, N. Tuccitto, D. Sapuppo, I.S. Gilmore, J. S. Sharp, J.L.S. Lee, T. Mouhib, A. Delcorte, Improving secondary ion mass spectrometry C-60(n+) sputter depth profiling of challenging polymers with nitric oxide gas dosing, Anal. Chem. 85 (2013) 5064–5070, https://doi.org/10.1021/ac4003535.
[14] S. Ninomiya, K. Ichiki, H. Yamada, Y. Nakata, T. Seki, T. Aoki, J. Matsuo, Precise and fast secondary ion mass spectrometry depth profiling of polymer materials with large Ar cluster ion beams, Rapid Commun. Mass Spectrom. 23 (2009) 1601–1606, https://doi.org/10.1002/rcm.4046.
[15] M.P. Seah, R. Havelund, I.S. Gilmore, Universal equation for argon cluster size-dependence of secondary ion spectra in sims of organic materials, J. Phys. Chem. C 118 (2014) 12862–12872, https://doi.org/10.1021/jp502646s.
[16] N. Winograd, Gas Cluster Ion Beams for Secondary Ion Mass Spectrometry, Annu. Rev. Anal. Chem. 11 (2018) 29–48, https://doi.org/10.1146/annurev-anchem-061516-045249.
[17] D.J. Graham, M.S. Wagner, D.G. Castner, Information from complexity: challenges of TOF-SIMS data interpretation, Appl. Surf. Sci. 252 (2006) 6860–6868, https://doi.org/10.1016/j.apsusc.2006.02.149.
[18] M. Holzweber, T. Heinrich, V. Kunz, S. Richter, C.-H.-H. Traulsen, C.A. Schalley, W.E.S. Unger, Principal component analysis (PCA)-assisted time-of-flight secondary-Ion mass spectrometry (ToF-SIMS): A versatile method for the investigation of self-assembled monolayers and multilayers as precursors for the bottom-up approach of nanoscaled devices, Anal. Chem. 86 (2014) 5740–5748, https://doi.org/10.1021/ac500059a.
[19] V. Spampinato, M.A. Parracino, R. La Spina, F. Rossi, G. Ceccone, Surface analysis of gold nanoparticles functionalized with thiol-modified glucose sams for biosensor applications, Front. Chem. 4 (2016) 1–12, https://doi.org/10.3389/fchem.2016.00008.
[20] K. Gajos, K. Awsiuk, A. Budkowski, Controlling orientation, conformation, and biorecognition of proteins on silane monolayers, conjugate polymers, and thermo-responsive.
[21] polymer brushes: investigations using TOF-SIMS and principal component analysis, Colloid Polym. Sci. 299 (2021) 385–405. https://doi.org/10.1007/s00396-020-04711-7.[21] X. Dong, A. Gusev, D. M. Hercules, Characterization of polysiloxanes with different functional groups by time-of-flight secondary ion mass spectrometry, J. Am. Soc. Mass. Spectrom. 9 (1998) 292-298. https://doi.org/10.1016/S1044-0305(98)00003-8.
[22] K. Fukukawa, M. Ueda, Recent development of photosensitive polybenzoxazoles, Polym. J. 38 (2006) 405–418, https://doi.org/10.1295/polymj.38.405.
[23] B. Fan, F. Liu, G. Yang, H. Li, G. Zhang, S. Jiang, Q. Wang, Dielectric materials for high-temperature capacitors, IET Nanodielectrics 1 (2018) 32–40, https://doi.org/10.1049/iet-nde.2018.0002.
[24] M. Tomikawa, Polyimides for Micro-electronics Applications in: B.P. Nandeshwarappa, Sandeep Chandrashekharappa (Eds.), Polyimides, IntechOpen, 2022. https://doi.org/10.5772/intechopen.99965.
[25] Z. Dong, Q. He, D. Shen, Z. Gong, D. Zhang, W. Zhang, T. Ono, Y. Jiang, Microfabrication of functional polyimide films and microstructures for flexible MEMS applications, Microsyst. Nanoeng. 9 (2023) 1–22, https://doi.org/10.1038/s41378-023-00503-5.